Iron-Sulfur Cluster Cysteine-to-Serine Mutants of *Anabaena* [2Fe-2S] Ferredoxin Exhibit Unexpected Redox Properties and Are Competent in Electron Transfer to Ferredoxin:NADP$^+$ Reductase†

John K. Hurley,§ Anne M. Weber-Main,‖ Anne E. Hodges,‖ Marian T. Stankovich,‖ Matthew M. Benning,⊥,# Hazel M. Holden,⊥,# Hong Cheng,# Bin Xia,# John L. Markley,# Carlos Genzor,▽ Carlos Gomez-Moreno,▽ Rameh Hafezi,§ and Gordon Tollin*,§

Department of Biochemistry, University of Arizona, Tucson, Arizona 85721, Department of Chemistry, University of Minnesota, Minneapolis, Minnesota 55455, Department of Biochemistry and Institute for Enzyme Research, University of Wisconsin, Madison, Wisconsin 53706, and Departamento de Bioquímica y Biología Molecular y Celular, Universidad de Zaragoza, E-50009 Zaragoza, Spain

Received August 12, 1997; Revised Manuscript Received September 29, 1997⊗

ABSTRACT: The reduction potentials and the rate constants for electron transfer (et) to ferredoxin:NADP$^+$ reductase (FNR) are reported for site-directed mutants of the [2Fe-2S] vegetative cell ferredoxin (Fd) from *Anabaena* PCC 7120, each of which has a cluster ligating cysteine residue mutated to serine (C41S, C46S, and C49S). The X-ray crystal structure of the C49S mutant has also been determined. The UV−visible optical and CD spectra of the mutants differ from each other and from wild-type (wt) Fd. This is a consequence of oxygen replacing one of the ligating cysteine sulfur atoms, thus altering the ligand → Fe charge transfer transition energies and the chiro-optical properties of the chromophore. Each mutant is able to rapidly accept an electron from deazariboflavin semiquinone (dRfH·) and to transfer an electron from its reduced form to oxidized FNR although all are somewhat less reactive (30−50%) toward FNR and are appreciably less stable in solution than is wt Fd. Whereas the reduction potential of C46S (−381 mV) is not significantly altered from that of wt Fd (−384 mV), the potential of the C49S mutant (−329 mV) is shifted positively by 55 mV, demonstrating that the cluster potential is sensitive to mutations made at the ferric iron in reduced [2Fe-2S] Fds with localized valences. Despite the decrease in thermodynamic driving force for et from C49S to FNR, the et rate constant is similar to that measured for C46S. Thus, the et reactivity of the mutants does not correlate with altered reduction potentials. The et rate constants of the mutants also do not correlate with the apparent binding constants of the intermediate (Fd_{red}:FNR_{ox}) complexes or with the ability of the prosthetic group to be reduced by dRfH·. Furthermore, the X-ray crystal structure of the C49S mutant is virtually identical to that of wt Fd. We conclude from these data that cysteine sulfur d-orbitals are not essential for et into or out of the iron atoms of the cluster and that the decreased et reactivity of these Fd mutants toward FNR may be due to small changes in the mutual orientation of the proteins within the intermediate complex and/or alterations in the electronic structure of the [2Fe-2S] cluster.

Ferredoxins (Fd)[1] comprise a class of low molecular mass (6−14 kDa), acidic electron transfer (et) proteins that contain one or more iron-sulfur clusters as prosthetic groups. The cluster irons are bridged by inorganic sulfur atoms and are ligated to the polypeptide backbone by the thiolate side chains of cysteine residues. Fds can be of the [2Fe-2S], [4Fe-4S], or [3Fe-4S] variety and have reduction potentials ranging from −600 to +200 mV (*1*−*3*). They function in photosynthetic et, nitrate reduction, and carbon and sulfur metabolism (*4*−*7*). The Fd from vegetative cells of the cyanobacterium *Anabaena* PCC 7120 contains a single [2Fe-2S] cluster in an 11 kDa peptide chain. This "plant-type" Fd has a one-electron reduction potential of −384 mV (vs SHE, pH 7.5, 4 °C; ref 8) and functions to transfer electrons from photosystem I to ferredoxin:NADP$^+$ reductase (FNR), which catalyzes the two-electron reduction of NADP$^+$ to NADPH:

$$2Fd_{red} + NADP^+ + H^+ \xrightarrow{FNR} 2Fd_{ox} + NADPH \quad (1)$$

Anabaena Fd has been cloned and overexpressed in *Escherichia coli* (*9*), and its three-dimensional structure has been solved at high resolution (*10*, *11*), thus making it a good candidate for studies of structure−function relationships in this ubiquitous and important class of redox proteins.

† This work has been supported by grants from the National Institutes of Health (DK15057 to G.T., GM29344 to M.T.S., GM30982 to H.M.H., and GM35976 to J.L.M) and from CICYT (BIO94-0621-CO2-01 to C.G.M.).

‡ Coordinates for the *Anabaena* ferredoxin mutant (C49S) crystal structure described herein have been deposited in the Protein Data Bank at Brookhaven National Laboratories, Upton, NY (filename 1QOA).

* To whom correspondence should be addressed. E-mail: tollin@biosci.arizona.edu. Fax: (520) 621-9288.

§ University of Arizona.

‖ University of Minnesota.

⊥ Institute for Enzyme Research, University of Wisconsin.

Department of Biochemistry, University of Wisconsin.

▽ Universidad de Zaragoza.

⊗ Abstract published in *Advance ACS Abstracts,* November 15, 1997.

[1] Abbreviations: dRf, 5-deazariboflavin; dRfH·, 5-deazariboflavin semiquinone; $E_1^{\circ\prime}$formal potential of first electron transfer; $E_2^{\circ\prime}$formal potential of second electron transfer; E_m, midpoint potential; et, electron transfer; Fd, ferredoxin; Fd_{ox}, oxidized ferredoxin; Fd_{red}, reduced ferredoxin; FNR, ferredoxin:NADP$^+$ reductase; FNR_{ox}, oxidized ferredoxin:NADP$^+$ reductase; FNR_{red}, reduced ferredoxin:NADP$^+$ reductase; MCD, magnetic circular dichroism; rms, root-mean-square; SHE, standard hydrogen electrode; wt, wild-type.

S0006-2960(97)02001-1 CCC: $14.00

The FNR from the closely related *Anabaena* PCC 7119 is a 36 kDa protein containing one FAD cofactor. It also has been cloned and overexpressed in *E. coli* (*12*−*14*) and has been structurally characterized by X-ray crystallography (*15*). The two-electron reduction potential of this recombinant FNR (E_m) is −323 mV, and the one-electron potentials of the oxidized/semiquinone (E_1^{ox}) and the semiquinone/reduced couples (E_2^{ox}) are −331 and −314 mV, respectively (*8*). Thus, both et steps from Fd to FNR are thermodynamically favorable in the physiological direction of electron flow. The driving force for et is further increased when Fd and FNR are bound in 1:1 electrostatic complexes, largely due to positive shifts in the reduction potentials of the reductase (*8*).

It has been established (*16*, *17*) that Fd and FNR react in a (minimal) two-step mechanism in which et follows complex formation, as depicted in eq 2:

$$Fd_{red} + FNR_{ox} \xrightarrow{K_d} (Fd_{red}{:}FNR_{ox}) \xrightarrow{k_{et}} Fd_{ox} + FNR_{red} \quad (2)$$

Early work suggested the involvement of both electrostatic and hydrophobic forces in the Fd/FNR interaction (*16*). This has been confirmed more directly in a recent study (*18*), which has demonstrated that hydrophobic interactions play a dominant role in causing the two proteins to become optimally oriented for et, whereas electrostatic forces can become inhibitory at low ionic strengths. Previous work from these laboratories has also examined how various site-specific mutations of Fd surface residues influence both the properties of the iron-sulfur protein and the Fd/FNR interaction (*8*, *17*, *19*, *20*). Three residues, S47, F65, and E94, have been shown to be crucial to the Fd/FNR interaction; in order to maintain efficient et to FNR, the residue at position 47 must bear a side-chain hydroxyl group (*8*), the residue at position 65 must be aromatic (*21*), and the residue at position 94 must be acidic (*22*). Interestingly, the same requirements hold for maintaining the negative reduction potential of the Fd (*8*).

As stated above, the iron-sulfur clusters of Fds are typically ligated to the polypeptide chain by cysteine thiolates. One notable exception is the [4Fe-4S] Fd from the hyperthermophile *Pyrococcus furiosus*, in which an aspartate residue has been identified as a ligand by ^{1}H NMR spectroscopy and inferred for other [4Fe-4S] Fds from sequence comparisons (*23*). In many [2Fe-2S] Fds, site-directed mutagenesis has been used to identify the amino acid ligands to the inorganic cluster (*24* and references therein), particularly in systems with greater than four cysteines in their primary sequences. However, in the *Anabaena* Fd sequence, a total of only four cysteines is present (C41, C46, C49, and C79), arranged in a C-X_4-C-X_2-C-X_{29}-C motif characteristic of "plant-type" Fds. These have been definitively identified as cluster ligands in the oxidized protein by X-ray crystallography (*10*, *11*). Furthermore, ^{1}H NMR experiments with the reduced Fd have shown that C41 and C46 ligate the localized Fe(II) site (iron 1), while C49 and C79 ligate the iron atom which remains Fe(III) (iron 2) (*25*).

In other classes of iron-sulfur proteins, naturally-occuring mixed ligation by sulfur and nitrogen or oxygen has been observed (*24*). For example, Rieske-type [2Fe-2S] clusters found in photosynthetic and respiratory electron transport chains and bacterial dioxygenases have two cysteine sulfurs and two histidine imidazole nitrogens in their coordination sphere (*26*−*30*), resulting in anomalous spectroscopic properties and high reduction potentials (−155 to +350 mV) compared to Fd [2Fe-2S] clusters with full cysteinal coordination. Mutagenesis coupled with extensive spectroscopic data has suggested one noncysteinal, oxygenic ligand for the [2Fe-2S] cluster of human ferrochelatase (*31*). In substrate-bound aconitase, the additional iron atom which converts the [3Fe-4S] form of the enzyme to the [4Fe-4S] form is coordinated by substrate carboxyl and hydroxyl oxygens and one solvent hydroxyl (*32*).

These discoveries of iron-sulfur proteins with noncysteinal ligation and the successful synthesis of [2Fe-2S] inorganic models with non-sulfur ligands (*33*, *34*) have encouraged the use of site-directed mutagenesis to create [2Fe-2S] proteins with mixed ligation. Werth et al. (*35*, *36*) have reported redox and EPR studies of Cys → Ser (or Asp) mutants of the FrdB subunit of *E. coli* fumarate reductase. These studies and the fact that the equivalent position in *E. coli* succinate dehydrogenase is occupied by an aspartate residue have demonstrated that oxygen can serve as a ligand to a [2Fe-2S] cluster without loss of activity. Site-directed mutagenesis experiments coupled with NMR, resonance Raman, and UV−visible spectroscopies have demonstrated serine ligation in both the Fd (*37*) and rubredoxin from *Clostridium pasteurianum* (*38*). The X-ray structure of a Cys → Ser mutant of *C. pasteurianum* rubredoxin [which has a Fe(S-Cys)$_4$ cluster] has also been reported (*39*).

For the *Anabaena* Fd, a previous study has shown that each of the four ligating cysteines can be individually replaced by serines using site-directed mutagenesis, and the resulting mutants have been characterized by optical, EPR, and ^{1}H NMR spectroscopy (*40*). Although the mutant Fds were less stable in solution than the wt protein, the cluster was clearly intact. Similarly, in human Fd, individual mutations of each of the ligating cysteines to serine resulted in [2Fe-2S] cluster formation under *in vitro* reconstitution conditions (*41*). These latter mutants were less stable than the corresponding mutations in *Anabaena* Fd, but were successfully characterized by UV−visible and EPR spectroscopies (*41*).

In the present study, we have continued the characterization of the Cys → Ser *Anabaena* Fd mutants, focusing primarily on their functional properties. We have evaluated the reduction potentials of the C46S and C49S mutants (the instability of C79S and of the reduced form of C41S precluded measurement of the potentials for these mutants) and have directly demonstrated that three of the mutants (C41S, C46S, and C49S) are active in et, both with FNR and with the nonphysiological donor deazariboflavin semiquinone, albeit with somewhat decreased rate constants relative to the wt protein (the instability of the C79S mutant precluded determination of its et properties). Also, the X-ray crystal structure of the C49S mutant has been determined at high resolution, thereby directly demonstrating the replacement of an Fe−S bond by an Fe−O bond, without a significant change in the geometry of the cluster. To our knowledge, this represents the first such structure for a [2Fe-2S] ferredoxin in which a native Cys ligand has been replaced by a Ser.

MATERIALS AND METHODS

Protein Preparation. Wt and mutant vegetative cell *Anabaena* Fds were prepared and characterized as described previously (*17*, *40*), as was native FNR (*42*).

Circular Dichroism Measurements. Circular dichroism spectra were measured in the visible and near-UV regions of the spectrum using an Aviv Model 60DS Spectropolarimeter (Aviv Assoc., Lakewood, NJ). Proteins were present at concentrations of 65−90 μM in 20 mM Tris buffer (pH 7.3) containing 100 mM NaCl. The spectra shown represent an average of four scans. UV−visible optical spectra confirmed that negligible degradation of the protein sample had occurred during the CD measurement.

Transient Kinetics. The laser flash photolysis system used for transient kinetic measurements consisted of a dye laser (BBQ 2A368 dye, 396 nm λ_{max}, 0.1 mJ energy), pumped by a PRA Model LN100 pulsed N_2 laser with 300 ps pulse duration (fwhm). The optical detection system was as described previously (*43*, *44*), except that the Nicolet 1170 signal averager has been replaced with a Tektronix TDS 410A digitizing oscilloscope in the present apparatus.

The photochemical reaction by which the 5-deazariboflavin (dRf) triplet state initiates protein−protein et has also been described (*45*−*47*). Briefly, the laser-generated dRf triplet state abstracts a hydrogen atom from a sacrificial donor (methionine was used in the present experiments in place of EDTA, because of cluster stability problems with the mutant Fds which were exacerbated when EDTA was used), which is present in 10-fold molar excess relative to the protein concentration. The resulting dRf semiquinone (dRfH•), in competition with its own disproportionation, reduces oxidized Fd. All kinetic experiments were performed at room temperature and under pseudo-first order conditions in which Fd is present in large excess over the dRfH• generated by the laser flash (<1 μM) (see ref 16 for additional details). Under these conditions, dRfH• reacts almost exclusively with oxidized Fd when both Fd and smaller amounts of FNR are present simultaneously (*16*). This allows the one-electron transfer from reduced Fd to oxidized FNR to be monitored. Solutions of dRf (95−100 μM in 4 mM phosphate buffer, pH 7.0, containing 1 mM methionine) were made anaerobic by bubbling for 1 h with H_2O-saturated argon. This solution was placed in a 1 cm cuvette, and microliter volumes of concentrated protein solutions were introduced through a rubber septum. Ar gas was blown over the sample surface to remove any added oxygen. Solution ionic strength was adjusted by anaerobic addition of small aliquots of 5 M NaCl. Generally, data from 4−8 laser flashes were averaged. Digitized kinetic traces were analyzed using a computer fitting routine (Kinfit, OLIS Co., Bogart, GA).

Spectroelectrochemical Titrations. All reduction potentials reported herein are relative to the standard hydrogen electrode (SHE). Reduction potentials for the mutants C46S and C49S were determined from potentiometric titrations using a three-electrode spectroelectrochemical cell previously described (*48*, *49*). For each experiment, a solution of 29−72 μM protein buffered at pH 7.5, 4 °C (50 mM potassium phosphate) containing 1 mM EDTA, 1 μM 5-deazaflavin (gift of Dr. Sandro Ghisla), and approximately 5 μM benzylviologen indicator dye (Sigma) was made anaerobic by repeated cycling of argon and vacuum over a 2 h period. Stepwise photoreduction, resulting in the production of the highly reductive deazaflavin semiquinone (*50*), was initiated by irradiating the solution with a 650 W projector bulb for 5−30 s per titration point. For each point, the system was allowed to equilibrate (approximately 30 min) while the solution was stirred in a temperature-controlled cell holder of a Perkin-Elmer 2S or 12S UV−visible spectrophotometer interfaced to an IBM-compatible computer. The solution potential was monitored using an Orion Research Model 601A digital ionanalyzer. When the potential remained stable within 1−2 mV for 10 min, it was recorded and a UV−visible spectrum was collected and stored. Upon reoxidation in air at the end of each experiment, >95% protein was recovered. Concentrations of oxidized and reduced Fd were quantitated from their spectra using Beer's law and the appropriate molar extinction coefficients (determined in this work from a combination of amino acid quantitation and spectroscopy): for C46S, $\epsilon_{ox,468nm} = 6300$ M^{-1} cm^{-1}, $\epsilon_{red,468nm} = 3400$ M^{-1} cm^{-1}; for C49S, $\epsilon_{ox,460nm} = 5350$ M^{-1} cm^{-1}, $\epsilon_{red,460nm} = 1700$ M^{-1} cm^{-1}. Prior to redox species quantitation, turbidity and dye contributions were subtracted out using the Perkin-Elmer PECSS program. Reduction potentials ($E^{\circ\prime}$) were calculated from a computerized nonlinear regression fit (*51*) to a plot of E vs [ox]/[red] according to the Nernst equation:

$$E = E^{\circ\prime} + (0.055/n)\log([ox]/[red])$$

where E is the measured equilibrium potential at each point in the titration and n is the number of electrons.

Crystallization, X-ray Data Collection, and Least-Squares Refinement. X-ray diffraction quality crystals of C49S were grown at 4 °C by the hanging drop method of vapor diffusion, as previously described (*10*). The precipitant solution typically contained 2.6 M ammonium sulfate, 50 mM potassium succinate (pH 5.5), and 1% 2-methyl-2,4-pentanediol. The crystals belonged to the space group $P2_12_12_1$ with unit cell dimensions of $a = 37.6$ Å, $b = 38.1$ Å, $c = 147.4$ Å, and two molecules per asymmetric unit. A complete X-ray data set for the C49S protein was collected from a single crystal at 4 °C with a Siemens X1000D area detector system. The X-ray source was nickel-filtered Cu Kα radiation from a Rigaku RU200 X-ray generator operated at 50 kV and 50 mA. The X-ray data were processed with the data reduction software package XDS (*52*, *53*) and internally scaled according to a procedure developed in the laboratory by Dr. Gary Wesenberg. Relevant X-ray data collection statistics are given in Table 1.

The structure of the mutant protein was solved by difference Fourier techniques, and the model was subjected to alternate cycles of least-squares refinement with the program TNT (*54*) and manual-model building with the software package, FRODO (*55*). During the refinement, the geometry of the [2Fe-2S] cluster was restrained to that observed in the small-molecule structural determination of $(Et_4N)_2[FeS(SCH_2)_2C_6H_4]_2$ by Mayerle et al. (*56*). Relevent refinement statistics can be found in Table 2. Figure 1 shows the electron density map in the vicinity of the mutated residue (S49) in this variant. In the X-ray structure, the iron ligated to residues 41 and 46 is designated as iron 1, and the iron ligated to residues 49 and 79 is designated as iron 2.

RESULTS AND DISCUSSION

We have previously described the successful creation, isolation, and biophysical characterization of four site-

Table 1: Intensity Statistics

	resolution range (Å)								
	overall	100.0−3.40	2.70	2.36	2.14	1.99	1.87	1.78	1.70
no. of measurements	58 282	13 383	9533	9125	8697	6314	3988	3764	3478
no. of independent reflections	21 258	2910	3004	3015	2890	2567	2383	2314	2175
% completeness	85	90	97	98	94	84	76	73	66
average intensity	3445	10 000	3976	1564	985	608	320	189	119
average sigma	124	287	147	80	65	52	36	31	28
R factor (%)[a]	2.9	2.4	3.0	4.5	5.2	5.8	6.9	8.8	10.5

[a] R factor $= (\Sigma|I - \bar{I}|/\Sigma I)100$.

Table 2: Refinement Statistics

resolution limits (Å)	30.0−1.70
R factor (%)[a]	18.2
no. of reflections used	20 713
no. of protein atoms	1508
no. of solvent atoms	114
weighted root-mean-square deviations from ideality	
bond length (Å)	0.014
bond angle (deg)	2.25
planarity (trigonal) (Å)	0.005
planarity (other planes) (Å)	0.008
torsional angle (deg)[b]	17.6

[a] R factor $= \Sigma|F_o - F_c|/\Sigma|F_o|$ where F_o is the observed structure-factor amplitude and F_c is the calculated structure-factor amplitude. [b] The torsional angles were not restrained during the refinement.

directed Fd mutants: C41S, C46S, C49S, and C79S (*40*). Here, we report on the functional properties of these mutants (i.e., their reduction potentials and kinetic constants for et from Fd_{red} to FNR_{ox}) and present an X-ray crystallographic structure for C49S.

Reduction potentials (E°′) for C46S and C49S (the only two mutants stable enough in their oxidized and reduced states to withstand the 8-h equilibrium experiments) were determined from potentiometric titrations (Figure 2, Table 3) and compared to that of wt Fd. Changing Cys to Ser at position 46 did not alter the reduction potential of the cluster, despite ^{1}H NMR evidence that the iron ligated by this residue (iron 1) is predominantly Fe(II) in both reduced wt Fd (*25*) and the reduced C46S mutant (*40*). For the mutants C46S and C41S, both of which involve a ligation change at iron 1, two distinct EPR signals with unique g_{av} values (1.91 and 1.95) have been detected in frozen samples of the reduced proteins. This suggests a mixture of two species: one in which iron 1, to which Ser is ligated, is Fe(II) and one in which iron 1 is Fe(III) (M. K. Johnson, personal communication). Although it is not reflected in the macroscopic cluster reduction potential of C46S, a shift in the relative potentials of the individual irons may have occured as a result of the mutation; presumably, the change from a sulfur to a more basic oxygen ligand at residue 46 would make this particular iron less reducible, inducing a corresponding change in the degree to which the reducing electron is localized on iron 1. Such an effect has been observed in the oxidized C77S mutant of the [4Fe-4S] high-potential iron protein (HiPIP) from *Chromatium vinosum*, in which the equilibrium between the Fe^{3+} and $Fe^{2.5+}$ states for the Ser-bound iron was found to shift in favor of the Fe^{3+} form compared to wt percentages (*57*). Reduced [2Fe-2S] clusters in proteins are almost exclusively valence localized, with an $S = 1/2$ antiferromagnetically coupled ground state. While it appears that significant direct Fe−Fe electronic coupling can provide a pathway for valence delocalization in [2Fe-2S] dimers, their large Heisenberg exchange coupling constants and the greater influence of vibronic coupling terms in $S = 1/2$ versus $S = 9/2$ states usually outweigh this electronic coupling (*58*). Nevertheless, the valence-delocalized $S = 9/2$ state has been detected in a few reduced [2Fe-2S] protein clusters, specifically the C60S and C56S mutants of the *C. pasteurianum* [2Fe-2S] Fd (*59*). For this system, a double exchange mechanism has been shown to be responsible for cancelling out some of the environmental differences between the two irons (*60*). For *Anabaena* C46S and C41S, it is not known definitively whether the mixture of species observed in frozen EPR samples of the reduced proteins exists at higher temperatures (as in our potentiometric experiments). If indeed present, these species are likely to be indistinguishable by simple UV−visible spectroscopy, so that the measured reduction potential reported here for C46S would reflect contributions from both. Additional experiments are necessary to further define the electronic properties of this mutant.

Replacement of Cys at residue 49 with a Ser shifted the potential 55 mV positively (Table 3), bringing it closer to the potentials of vertebrate Fds such as bovine adrenodoxin (−270 mV, pH 7.0, ref 61) and human Fd (−260 mV, pH 7.4; A. M. Weber-Main, M. T. Stankovich, and L. E. Vickery, unpublished data). Mutation from a sulfur to an oxygen ligand at residue 49 would likely make iron 2 less reducible in this variant; however, since iron 2 remains ferric in reduced wt Fd, this mutation would not be expected to change the site of electron localization. Indeed, EPR, resonance Raman, and MCD data obtained for the *Anabaena* C49S mutant are indicative of Ser coordinating at the Fe(III) site of the reduced cluster, as for the Cys in the wt Fd (M. K. Johnson, personal communication). Taken in combination, these results demonstrate that the reduction potentials of [2Fe-2S] clusters can be sensitive to the nature of the ligands at the nonreducible iron. Similarly, the C65S mutation in fumarate reductase [presumedly an Fe(III) ligand in the reduced enzyme] has been shown to shift the [2Fe-2S] center potential 30 mV positively (*35*). At this time, it is unclear what is inducing the large positive potential shift in this fairly conservative mutant. We have found shifts of this direction and magnitude (and greater) in nonconservative Fd mutations which disrupt hydrogen-bonding to the [2Fe-2S] cluster or remove aromaticity or negative charges at the protein surface (*8*). We have previously shown that the reduced C49S mutant differs dramatically from wild-type in its biophysical properties (*40*); both its EPR spectrum (axial rather than rhombic) and its pattern of hyperfine shifted peaks in the ^{1}H NMR spectrum more closely resemble those of the vertebrate class of [2Fe-2S] Fds than those of plant-type Fds. Furthermore, the visible spectrum of reduced C49S is characterized by a prominent new peak at approximately

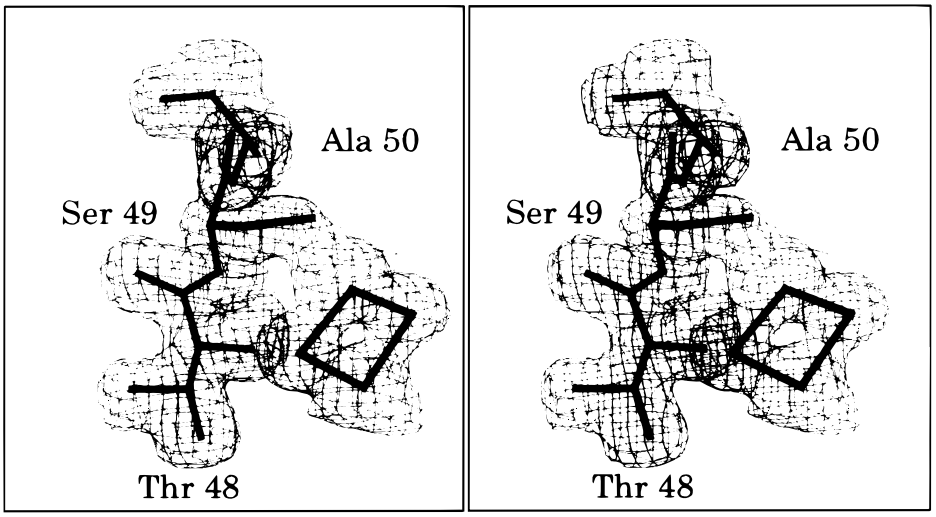

FIGURE 1: Electron density map of the C49S mutant in the vicinity of the mutated residue. The electron density shown was calculated to 1.7 Å resolution with coefficients of the form $(2F_0 - F_C)$, where F_0 and F_C were the native and calculated structure factor amplitudes, respectively. The map was contoured at 1σ. The figure was prepared with the software package, FROST, written by Dr. Gary Wesenberg, University of Wisconsin.

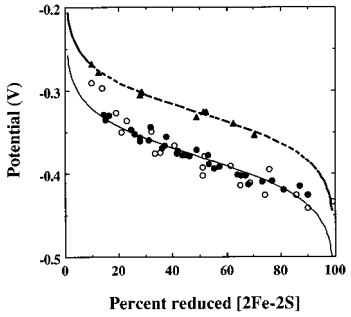

FIGURE 2: Plot of reduction potential versus the percent reduced [2Fe-2S] in wt and the mutants C46S and C49S from *Anabaena* vegetative Fd. Data were collected during spectroelectrochemical titrations as reported in Materials and Methods: wild-type Fd (●); C46S (○); C49S (▲). The theoretical curves deduced from the spectroelectrochemically determined reduction potentials for $n = 1$ systems are plotted: wt (solid line); C49S (dotted line). The C46S curve superimposes that of wt and, thus, was not included in this figure.

Table 3: Kinetic and Thermodynamic Parameters for Wild-Type and Cys → Ser Mutants of *Anabaena* Vegetative Ferredoxin[a]

Fd	$k_{dRfH} \times 10^{-8}$ $(M^{-1}\,s^{-1})$[b]	k_{et-FNR} (s^{-1})[c]	K_d (μM)[c]	$E^{\circ\prime}$ (mV)
wt	2.0 ± 0.2	6200 ± 400[d]	9.3 ± 0.7[d]	-384 ± 1[e]
C41S	1.0 ± 0.1	3000 ± 400	15.0 ± 2.2	*f*
C46S	1.9 ± 0.1	1900 ± 150	14.5 ± 1.1	-381 ± 3
C49S	1.6 ± 0.1	2200 ± 200	3.0 ± 0.6	-329 ± 1

[a] Reactions were carried out at an ionic strength of 100 mM. For the determination of second-order rate constants, typically 5−6 protein concentrations over the range 5−40 mM were used. [b] Rate constants for the reduction of Fd by dRfH•. [c] Rate constants for et from reduced Fd to oxidized FNR and K_d values for the transient (Fd_{red}:FNR_{ox}) complex were calculated from the data in Figure 4 as described in the text. [d] Taken from ref 18. [e] Taken from ref 8. [f] The instability of the reduced form of C41S precluded the measurement of its reduction potential.

550 nm (data not shown), a feature unique to vertebrate Fds as well as the as yet "unclassified" Fd from *E. coli* ($E^{\circ\prime} \approx -350$ mV; A. M. Weber-Main, M. T. Stankovich, and L. E. Vickery, unpublished data). These observations suggest a distinct electron distribution within the reduced [2Fe-2S] cluster of C49S which may be common to the vertebrate class of Fds and which is manifested in both the spectroscopic and redox properties of the chromophore. In addition to thermodynamic parameters, transient kinetic data were collected to characterize the ability of these mutants to transfer reducing equivalents to FNR, the biological partner of Fd, and to accept electrons from dRfH•. Upon laser flash excitation of a deoxygenated solution containing dRf, methionine, oxidized Fd (wt or mutant), and FNR, the dRf triplet state extracts a hydrogen atom from methionine in <1 μs, generating dRfH•, which then reduces Fd (*17*). As Table 3 shows, dRfH• reacts with each of the Cys → Ser mutants with a rate constant that is within a factor of 2 of wt Fd. This has also been found to be true of all other Fd mutants studied to date (*8*, *17*, *19*, *20*) and has been taken as evidence that the [2Fe-2S] center remains accessible and redox active in the mutant proteins.

The Fd_{red} which is formed in this reaction is able to reduce FNR_{ox} (cf., refs 46 and 47 for a discussion of this reaction scheme). We have recently shown that only free FNR_{ox} is capable of being reduced in this system, i.e., that a preformed complex of the oxidized proteins (Fd_{ox}:FNR_{ox}) cannot be reduced by either Fd_{red} or dRfH•, presumably because of steric effects (*18*). Figure 3 shows kinetic traces demonstrating the formation of the FNR semiquinone due to the reaction between FNR_{ox} and Fd_{red} for wt Fd and for the mutants C41S, C46S, and C49S. The production of the semiquinone form of FNR can be monitored at 600 nm. As is evident from these data, all of the mutants are significantly reactive with FNR. Although not shown in Figure 3, the oxidation of Fd_{red} can be monitored at 507 nm (*17*), which is an isosbestic point for the FNR semiquinone. As expected, the rate constants of Fd_{red} oxidation and FNR_{ox} reduction determined at these two wavelengths are the same within experimental error (data not shown). These reactions were carried out at an ionic strength of 100 mM for two reasons. First, the Fd mutants investigated in this study had increased stability at high salt concentrations. Second, as has been observed previously (*8*, *17*, *18*), the dependence of k_{obs} on FNR concentration (see below), which is linear at low ionic strength (12 mM), shows curvature at high ionic strength (100 mM), thereby allowing direct measurements of both K_d and k_{et} (see eq 2 above).

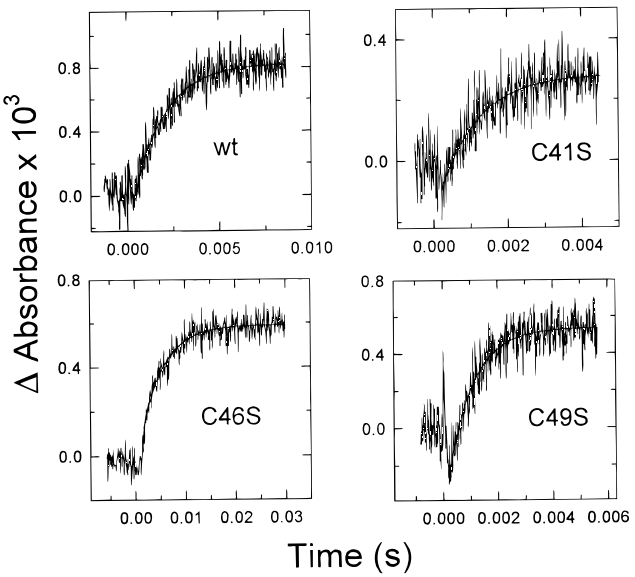

FIGURE 3: Transient kinetic curves demonstrating the reduction of FNR to its semiquinone form by reduced Fd for wt and Cys → Ser mutants of *Anabaena* Fd. The monitoring wavelength was 600 nm. The experiment with wt Fd used 30 μM Fd and 5 μM FNR; that with C41S used 40 μM Fd and 10 μM FNR; the experiments with C46S and C49S each used 40 μM Fd and 5 μM FNR. Solutions also contained 1 mM methionine and 95−100 μM dRf in 4 mM potassium phosphate buffer (pH 7.0). Solid lines are monoexponential fits to the data.

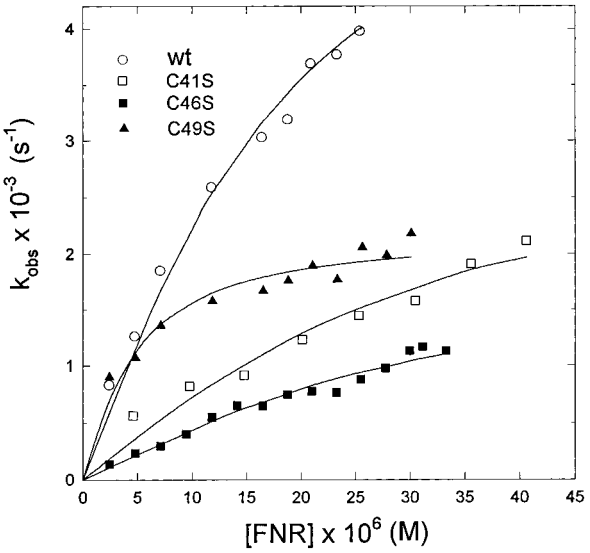

FIGURE 4: FNR concentration dependence of the pseudo-first-order rate constants for the reduction of FNR by wt and Cys → Ser mutants of *Anabaena* vegetative cell Fd at 100 mM ionic strength. Fd concentrations were 40, 55, 48, and 73 μM for the wt Fd, C41S, C46S, and C49S experiments, respectively. Solid lines through the data are theoretical fits to the data assuming a two-step mechanism as described in the text. Solutions were buffered at pH 7.0 with 4 mM potassium phosphate. The ionic strength was adjusted using aliquots of 5 M NaCl.

This is due to the increased concentration of the preformed (Fd_{ox}:FNR_{ox}) complex at low ionic strength; because this complex cannot be reduced by either dRfH· or Fd_{red}, it requires higher concentrations of FNR than are experimentally accessible to show saturation effects. It should be noted that, whereas correcting the kinetic plots for the concentration of FNR existing as preformed complex results in an appreciable lowering of the K_d value, it produces no significant change in the k_{et} value (*18*). The latter is the parameter of significance in the present study.

For the reaction mechanism given in eq 2, the dependence of the observed rate constant (k_{obs}) on FNR concentration should be hyperbolic as the rate-limiting step switches from complex formation to et. When such saturation kinetics are obtained, fitting the data to the exact solution of the differential equations describing this mechanism yields values for k_{et} and for the dissociation constant (K_d) of the intermediate (Fd_{red}:FNR_{ox}) complex (*62*, *63*). As has been noted previously (*47*), k_{et} reflects any and all processes which are associated with the attainment of the transition state for the transfer of an electron, including structural changes in the protein or structural rearrangements occurring within the transient et complex (conformational gating), and changes in hydration of functional groups and not necessarily the actual electron transfer event itself.

As shown in Figure 4, the wt Fd and the C41S, C46S, and C49S mutants exhibit such saturation kinetics (although the nonlinearity for C41S and C46S is not as pronounced as for the C49S mutant, implying a larger value for K_d). The k_{et} and K_d values derived from these curves are given in Table 3. It is apparent that all of the mutants bind to FNR and have appreciable rates of et, although k_{et} is significantly smaller (30−50%) for all of the mutants relative to wt Fd. The observed decreases in k_{et} values cannot be ascribed to alterations in the reduction potentials of the mutants, inasmuch as k_{et} for the C49S protein, which has a potential 55 mV higher than wt Fd, is comparable to that for the C46S mutant, which has the same reduction potential as wt Fd. Moreover, despite the greater than 50 mV positive potential shift in the C49S mutant, et from the Fd to FNR is still isopotential and thus thermodynamically feasible [the one-electron reduction potential for the oxidized/semiquinone form of FNR is −331 mV (8)]. The K_d values [for the transient (Fd_{red}:FNR_{ox}) complex] for the C41S and C46S mutants are slightly larger than that of wt Fd, whereas the K_d for C49S is significantly smaller. Thus, et reactivity does not correlate with the binding constant of the transient (Fd_{red}:FNR_{ox}) complex either, as is seen also with other Fd mutants (*8*, *20*). The changes in K_d values for the Cys → Ser mutants correlate with their location in the cluster; C41S and C46S, which have larger K_d values than wt Fd, are at the front surface of the cluster (exposed to the solvent), whereas C49S, which has a 3-fold smaller K_d value than wt, is at the back of the cluster and buried within the protein interior. It is not clear why mutation of this buried residue affects K_d, particularly in view of the absence of structural perturbations resulting from the mutation (see below). This might involve changes in the electronic structure of the [2Fe-2S] cluster, which are also reflected in the 55 mV positive shift of the reduction potential (Table 3) and in the altered CD spectrum (see below) of the C49S mutant.

The X-ray crystal structure of the C49S mutant revealed no gross structural perturbations. Figure 5 a shows the C^{α} backbone of the mutant superimposed with that of wt Fd. The rms deviation is 0.132 Å. Figure 5b presents a close-up view of the wt and mutant proteins in the immediate vicinity of the [2Fe-2S] cluster, showing the C49 and S49 side chains and the remaining three cysteine ligands. Again, no large structural differences are detectable. The observed Fe−O bond distance of 2.0 Å in C49S, as compared with an Fe-S bond in the wt protein of 2.3 Å, clearly demonstrates

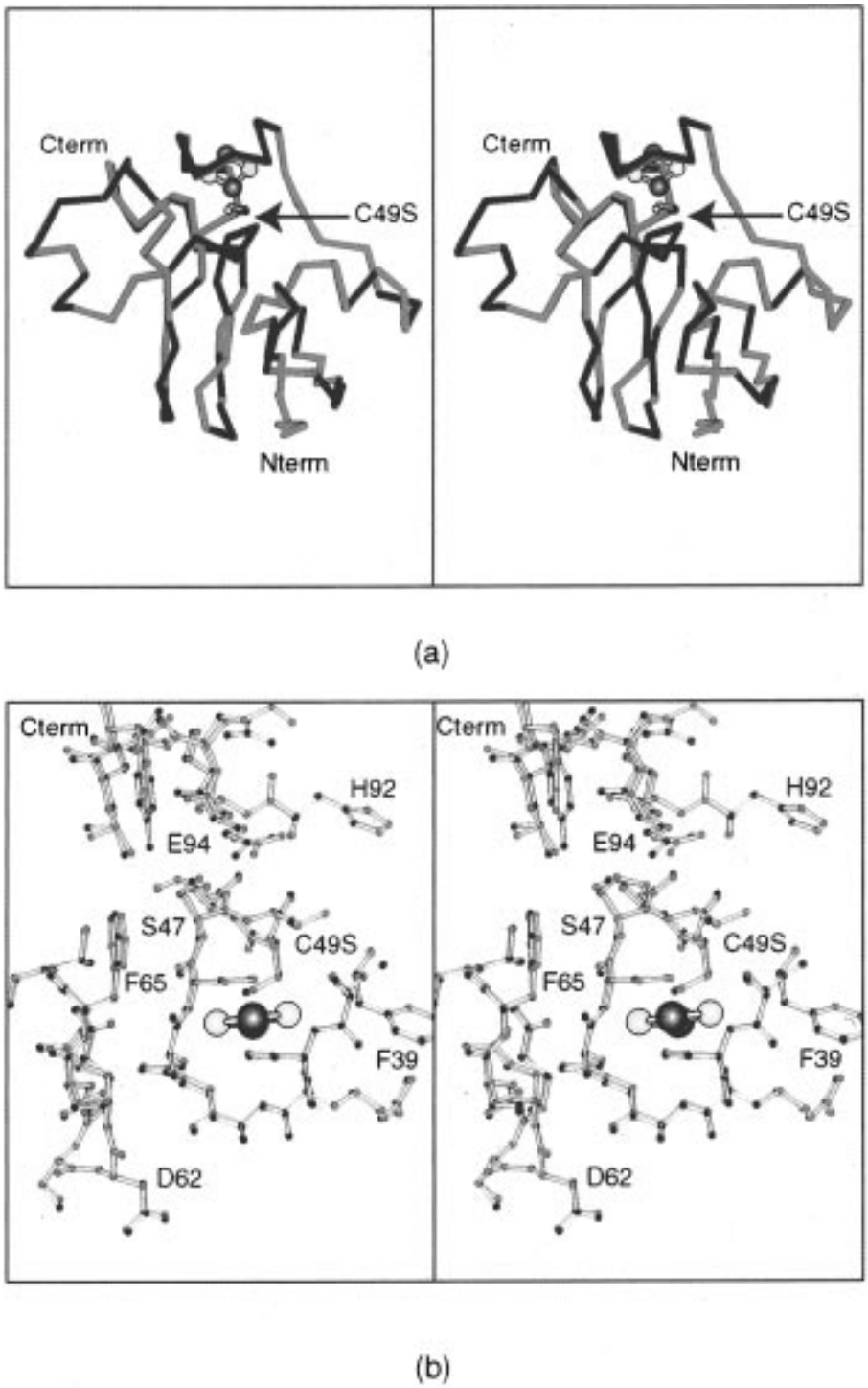

FIGURE 5: (a) Superposition of the C^{α} backbones of the wt (black) and C49S mutant (red) Fd. (b) Close-up view of the vicinity of the [2Fe-2S] cluster showing the mutated S49 side chain and side chains of the remaining three ligating cysteines. Wt and mutant proteins are differentiated as in the upper panel. The figures were prepared using MOLSCRIPT (*65*).

that Fe and O are bonded directly, without an intervening hydrogen. It is interesting to note the similarity observed in the structure of the C42S mutant of *C. pasteurianum* rubredoxin (*39*), which has an Fe−O bond length of 1.9 Å, approximately 0.4 Å shorter than the Fe−S bond in the native protein.

The immediate environment of the [2Fe-2S] cluster is a major determinant of the UV−visible spectral properties of the protein. As noted previously (*40*), the visible spectra of the Cys → Ser mutants are different from each other and from the wt protein. Figure 6 shows the optical absorption spectra of the wt and mutant Fds superimposed on the UV−visible CD spectra of the proteins. As expected, the CD spectra of the mutants are also dramatically different from one another and from wt Fd. This is clearly a consequence of perturbations of the electronic character of the [2Fe-2S] cluster in the mutants, which, as noted above, is not reflected in the 3-D structure of the protein. These spectral perturbations most likely result from altered symmetry in the [2Fe-2S] cluster and to the different energies of the ligand → Fe charge transfer transitions, caused by the substitution of oxygen for sulfur as one of the cluster ligands (*64*). These electronic alterations in the iron-sulfur cluster may be a factor in causing the changes in the protein−protein et kinetics of

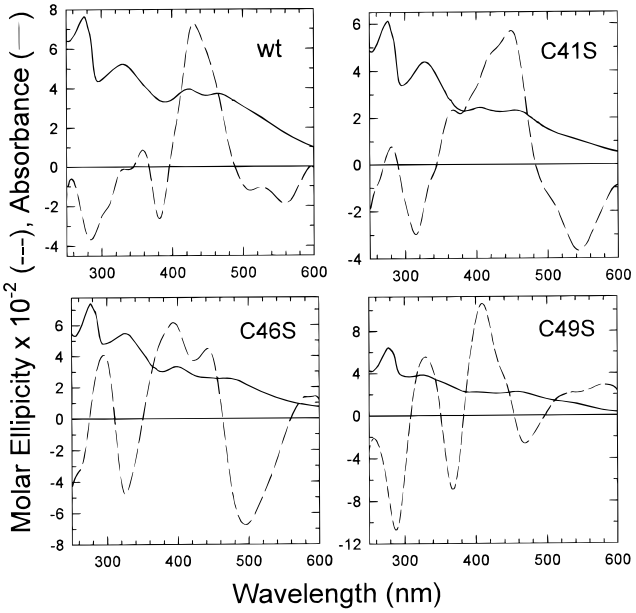

FIGURE 6: UV−visible and visible/near-UV circular dichroism spectra of wt and Cys → Ser mutants of *Anabaena* Fd. The UV−visible spectra have been adjusted such that A_{422} is equal to what it would be if the mutants were at a concentration of 20.6 μM, the concentration at which the spectrum of the wt protein was taken and then scaled up by a factor of 20 for purposes of comparison with the CD spectra. For the UV−visible spectra, proteins were present at the following concentrations: wt, 20.6 μM; C41S, 17.7 μM.; C46S, 14.5 μM; and C49S, 25.2 μM. For the CD spectra (average of four scans), proteins were present at the following concentrations: wt, 87.1 μM; C41S, 66.4 μM; C46S, 65.5 μM; and C49S, 66.3 μM. All solutions (for both UV−visible and CD analyses) also contained 100 mM NaCl in 20 mM Tris buffer (pH 7.3).

the mutants, and the altered FNR binding constant and reduction potential of the C49S mutant. Furthermore, as we have shown recently (*8*, *18*), the mutual orientation of Fd and FNR in the transient et complex is a major factor in determining et reactivity. Thus, the optimal prosthetic group orientation which exists in the wt (Fd_{red}:FNR_{ox}) complex may be less than optimal for the Cys → Ser mutant complexes, thereby altering the et kinetics. The observation that all of the Cys → Ser mutants are appreciably reactive in et suggests that Cys sulfur d-orbitals are not required for the transfer process to or from the iron atom. This deserves further study, perhaps using mutants in which more than one Cys has been converted to Ser, if these are stable enough to study. In any event, the present results support the idea that cysteines (rather than serine) have been chosen to serve as ligands to the [2Fe-2S] cluster in plant-type ferredoxins both because of enhanced cluster stability in both the oxidized and reduced forms (*40*) and because the cysteine-ligated cluster is more efficient in et to FNR. It will be interesting to determine whether or not the latter is also true for the other physiological redox partners of Fd.

REFERENCES

1. Cammack, R. (1984) in *Charge and Field Effects in Biosystems* (Allen, M. J., and Usherwood, P. R. N., Eds.) pp 41−51, Abacus Press, Tunbridge Wells.
2. Berg, J. M., and Holm, R. H. (1982) in *Iron-Sulfur Proteins* (Spiro, T. G., ed.), pp. 1−66, Wiley Interscience Publications, NY.
3. Arnon, D. I., and Buchanan, B. B. (1971) *Methods Enzymology 23,* 413−440.
4. Knaff, D. B. (1996) in *Oxygenic Photosynthesis: The Light Reactions* (Ort, D. R., and Yocum, C. F., Eds.) pp 333−361, Kluwer Academic Publishers, The Netherlands.
5. Knaff, D. B., and Hirasawa, M. (1991) *Biochim. Biophys. Acta 1056*, 93−125.
6. Lovenberg, W., Ed. (1973, 1977) *Iron-Sulfur Proteins*, Vol. 1 and 2 (1973), Vol. 3, (1977), Academic Press, New York.
7. Spiro, T. G., Ed. (1982) *Iron-Sulfur Proteins*, Vol. 4, Academic Press, New York.
8. Hurley, J. K., Weber-Main, A. M., Stankovich, M. T., Benning, M. M., Thoden, J. B., Vanhooke, J. L., Holden, H. M., Chae, Y. K., Xia, B., Cheng, H., Markley, J. L., Martínez-Júlvez, M., Gomez-Moreno, C., Schmeits, J. L., and Tollin, G. (1997) *Biochemistry 36*, 11100−11117.
9. Alam, J., Whitaker, R. A., Krogman, D. W., and Curtis, S. E. (1986) *J. Bacteriol. 168*, 265−1271; Böhme, H., and Hazelkorn, R. (1989) *Plant Mol. Biol. 12*, 667−672.
10. Rypniewski, W. R., Breiter, D. R., Benning, M. M., Wesenberg, G., Oh, B.-H., Markley, J. L., Rayment, I., and Holden, H. M. (1991) *Biochemistry 30*, 4126−4131.
11. Holden, H. M., Jacobson, B. L., Hurley, J. K., Tollin, G., Oh. B.-H., Skjeldal, L., Chae, Y. K., Cheng, H., Xia, B., and Markley, J. L. (1994) *J. Bioenerg. Biomembr. 26*, 67−88.
12. Fillat, M. F., Borrias, W. E., and Weisbeek, P. J. (1991) in *Flavins and Flavoproteins 1990* (Curti, B., Ronchi, S., and Zanetti, G., Eds.) pp 445−448, Walter de Gruyter and Co., Berlin.
13. Fillat, M. F., Pacheco, M. L., Peleato, M. L., and Gomez-Moreno, C. (1994) in *Flavins and Flavoproteins 1993* (Yagi, K., Ed.) pp 447−450, Walter de Gruyter and Co., Berlin.
14. Gomez-Moreno, C., Martinez-Júlvez, M., Fillat, M. F., Hurley, J. K., and Tollin, G. (1995) in *Photosynthesis: from Light to Biosphere* (Mathis, P., Ed.) Vol. II, pp 627−632, Kluwer Academic Publishers, The Netherlands.
15. Serre, L., Vellieux, F., Medina, M., Gomez-Moreno, C., Fontecilla-Camps, J., and Frey, M. (1996) *J. Mol. Biol. 263*, 20−39.
16. Walker, M. C., Pueyo, J. J., Navarro, J. A., Gomez-Moreno, C., and Tollin, G. (1991) *Arch. Biochem. Biophys. 287*, 351−358.
17. Hurley, J. K., Salamon, Z., Meyer, T. E., Fitch, J. C., Cusanovich, M. A., Markley, J. L., Cheng, H., Xia, B., Chae, Y. K., Medina, M., Gomez-Moreno, C., and Tollin, G. (1993) *Biochemistry 32*, 9346−9354.
18. Hurley, J. K., Fillat, M. F., Gomez-Moreno, C., and Tollin, G. (1996) *J. Am. Chem. Soc. 118*, 5526−5531.
19. Hurley, J. K., Fillat, M., Gomez-Moreno, C., and Tollin G. (1995) *Biochimie 77*, 539−548.
20. Hurley, J. K., Schmeits, J. L., Genzor, C., Gomez-Moreno, C., and Tollin, G. (1996) *Arch. Biochem. Biophys. 333*, 243−250.
21. Hurley, J. K., Cheng, H., Xia, B., Markley, J. L., Medina, M., Gomez-Moreno, C., and Tollin, G. (1993) *J. Am. Chem. Soc. 115*, 11698−11701.
22. Hurley, J. K., Medina, M., Gomez-Moreno, C., and Tollin, G. (1994) *Arch. Biochem.Biophys. 312*, 480−486.
23. Calzolai, L., Gorst, C. M., Zhao, Z.-H., Teng, Q., Adams, M. W. W., and La Mar, G. (1995) *Biochemistry 34*, 11373−11384.
24. Moulis, J-M, Davasse, V., Golinelli, M-P, Meyer, J., and Quinkal, I. (1996) *J. Biol. Inorg. Chem. 1*, 2−14.
25. Skjeldal, L, Westler, W. M., Oh, B.-H., Krezel, A. M., Holden, H. M., Jacobson, B. L., Rayment, I., and Markley, J. L. (1991) *Biochemistry 30*, 7363−7368.
26. Iwata, S., Saynovits, M., Link, T. A., and Michel, H. (1996) *Structure 4*, 567−579.
27. Davidson, E., Ohnishi, T., Tokito, M., Emmanuel, A.-A.-A., and Daldal, F. (1992) *Biochemistry 31*, 3342−3351
28. Gurbiel, R. J., Batie, C. J., Sivaraja, M., True, A. E., Fee, J. A., Hoffman, B. M., and Ballou, D. P. (1989) *Biochemistry 28*, 4861−4871.
29. Gurbiel, R. J., Ohnishi, T., Robertson, D. E., Daldal, F., and Hoffman, B. M. (1991) *Biochemistry 30*, 11579−11584.
30. Britt, R. D., Sauer, K., Klein, M. P., Knaff, D. B., Kriauciunas, A., Yu, A., Yu, L., and Malkin, R. (1991) *Biochemistry 30*, 1892−1901.

31. Crouse, B. R., Sellers, V. M., Finnegan, M. G., Dailey, H. A., and Johnson, M. K. (1996) *Biochemistry 35*, 16222−16229.
32. Lauble, H., Kennedy, M. C., Beinert, H., and Stout, C. D. (1992) *Biochemistry 31*, 2735−2748.
33. Mascharak, P. K., Papefthymiou, G. C., Frankel, R. B., and Holm, R. H. (1981) *J. Am. Chem. Soc. 103*, 6110−6116.
34. Beardwood, P., Gibson, J. F., Johnson, C. E., and Rush, J. D. (1982) *J. Chem. Soc., Dalton Trans.* 2015−2020
35. Werth, M. T., Cecchini, G., Manodori, A., Ackrell, B. A. C., Schröder, I., Gunsalus, R. P., and Johnson, M. K. (1990) *Proc. Natl. Acad. Sci. U.S.A. 87*, 8965−8969.
36. Werth, M. T., Sices, H., Cecchini, G., Schröder, I., Lasage, S., Gunsalus, R. P., and Johnson, M. K. (1992) *FEBS Lett. 299*, 1−4.
37. Meyer, J., Fujinaga, J., Gaillard, J., and Lutz, M. (1994) *Biochemistry 33*, 13642−13650.
38. Meyer, J., Gaillard, J., and Lutz, M. (1995) *Biochem. Biophys. Res. Comm. 212*, 827−833.
39. Ayhan, M., Xiao, Z, Lavery, M. J., Hammer, A. M., Scrofani, S. D. B., and Wedd, A. G., (1996) in *Transition Metal Sulfur Chemistry*, *ASC Symposium Series* (Stiefel, E. I., and Matsumoto, K., Eds.) Vol. 653, pp 40−56, American Chemical Society, Washington, DC.
40. Cheng, H., Xia, B., Reed, G. H., and Markley, J. M. (1994) *Biochemistry 33*, 3155−3164.
41. Xia, B., Cheng, H., Bandarian, V., Reed, G. H., and Markley, J. L. (1996) *Biochemistry 35*, 9488−9495.
42. Pueyo, J. J., and Gomez-Moreno, C. (1991) *Prep. Biochem. 21*, 191−204.
43. Przysiecki, C. T., Bhattacharyya, A. K., Tollin, G., and Cusanovich, M. A. (1985) *J. Biol. Chem. 260*, 1452−1458
44. Bhattacharyya, A. K., Tollin, G., Davis, M., and Edmondson, D. E. (1983) *Biochemistry 22*, 5270−5279.
45. Tollin, G. (1995) *J. Bioenerg. Biomembr. 27*, 303−309.
46. Tollin, G., and Hazzard, J. H. (1991) *Arch. Biochem. Biophys. 287*, 1−7.
47. Tollin G., Hurley, J. K., Hazzard, J. T., and Meyer, T. (1993) *Biophys. Chem. 48*, 259−279.
48. Stankovich, M. T. (1980) *Anal. Biochem. 109*, 295−308.
49. Stankovich, M. T., and Fox, B. (1983) *Biochemistry 22*, 4466−4472.
50. Massey, V., and Hemmerich, P. (1978) *Biochemistry 17*, 9−16.
51. Duggleby, R. G. (1981) *Anal. Biochem. 110*, 9−18.
52. Kabsch, W. (1988) *J. Appl. Crystallogr. 21*, 67−71.
53. Kabsch, W. (1988) *J. Appl. Crystallogr. 21*, 916−924.
54. Tronrud, D. E., Ten Eyck, L. F., and Matthews, B. W. (1987) *Acta Crystallogr., Sect. A.* 43, 489−501.
55. Jones, T. A. (1985) *Methods Enzymol. 115*, 157−171.
56. Mayerle, J. J., Frankel, R. B., Holm, R. H., Ibers, J. A., Phillips, W. D., and Weiher, J. F. (1973) *Proc. Natl. Acad. Sci. U.S.A. 70*, 2429−2433.
57. Babini, E., Bertini, I., Borsari, M., Capozzi, F., Dikiy, A., Eltis, L. D., and Luchinat, C. (1996) *J. Am. Chem. Soc. 118*, 75−80.
58. Gamelin, D. R., Bominaar, E. L., Kirk, M. L., Wieghardt, K., and Solomon, E. I. (1996) *J. Am. Chem. Soc. 118*, 8085−8097.
59. Crouse, B. R., Meyer, J., and Johnson, M. K. (1995) *J. Am. Chem. Soc. 117*, 9612−9613.
60. Achim, C., Golinelli, M.-P., Bominaar, E. L., Meyer, J., and Münck, E. (1996) *J. Am. Chem. Soc. 118*, 8168−8169.
61. Huang, J. J., and Kimura, T. (1973) *Biochemistry 12*, 406−409.
62. Simondsen, R. P., Weber. P. C., Salemme, F. R., and Tollin, G. (1982) *Biochemistry 21*, 6366−6375.
63. Simondsen, R. P., and Tollin, G. (1983) *Biochemistry 22*, 3008−3016.
64. Noodleman, L., and Baerends, E. J. (1984) *J. Am. Chem. Soc. 106*, 2316−2327.
65. Kraulis, P. J. (1991) *J. Appl. Crystallogr. 24*, 946−950.

BI972001I